



UDC 62-405.8

<https://doi.org/10.17073/1997-308X-2024-2-61-70>Research article
Научная статья

Transforming stereolithographic prototypes into metal or ceramic models by polymer substitution with titanium powder

M. A. Markov[✉], S. A. Cherebylo, E. V. Ippolitov, S. V. Kamaev,
M. M. Novikov, V. V. Vnuk

National Research Centre “Kurchatov Institute”
1 Kurchatov Sq., Moscow 123182, Russia

✉ Lc250@mail.ru


Abstract. The presented paper experimentally demonstrates the potential expansion of stereolithographic prototype utilization. Two methods for manufacturing plastic prototypes are proposed, enabling the subsequent substitution of the polymer material with either metal or ceramics. The first method involves additional actions by the prototype designer during the modeling stage. The second method necessitates alterations in the technological processes of model preparation and prototype manufacturing using a stereolithography apparatus. Material substitution occurs in two stages. Initially, cavities in the prototype are filled with powder material or a mixture of powder and water. Although titanium powder was chosen as the test material, the proposed technology permits the utilization of a broad spectrum of powder materials, encompassing both metallic and ceramic options. The subsequent stage involves heat treatment, where the polymer is eliminated, and the metal powder is sintered while retaining the original shape and dimensions of the prototype. Heat treatment of the acquired prototypes was conducted in both argon and atmospheric air environments. The utilization of different gas media might induce chemical transformations in the material filling the prototype. The experiments lead to the conclusion that the proposed approaches show promise and merit further development. Additionally, we contemplate amalgamating the two methods in the future to attain an optimized final outcome. The data we have gathered could significantly contribute to broadening the scope of stereolithography applications, given that this technology presently represents one of the most precise, widespread, and accessible additive manufacturing methods.

Keywords: additive technologies, titanium powder, 3D part, sintering

Acknowledgements: The study was conducted within the framework of the state assignment NRC “Kurchatov Institute”.

For citation: Markov M.A., Cherebylo S.A., Ippolitov E.V., Kamaev S.V., Novikov M.M., Vnuk V.V. Transforming stereolithographic prototypes into metal or ceramic models by polymer substitution with titanium powder. *Powder Metallurgy and Functional Coatings*. 2024;18(2):61–70. <https://doi.org/10.17073/1997-308X-2024-2-61-70>

Преобразование стереолитографических прототипов в металлические или керамические модели замещением полимера порошковым титаном

М. А. Марков , С. А. Черобыло, Е. В. Ипполитов, С. В. Камаев,
 М. М. Новиков, В. В. Внук

Федеральное государственное бюджетное учреждение
 «Национальный исследовательский центр «Курчатовский институт»
 Россия, 123182, г. Москва, пл. Академика Курчатова, 1

 Lc250@mail.ru

Аннотация. В работе экспериментально подтверждена возможность расширения области использования стереолитографических прототипов. Предложены два способа изготовления пластиковых прототипов, позволяющие впоследствии заместить полимерный материал моделей на металл или керамику. Первый из рассмотренных способов предполагает дополнительные действия конструктора, проектирующего прототип на стадии моделирования, второй – заключается во внесении изменений в технологические процессы подготовки модели и изготовления прототипа на стереолитографической установке. Замещение материала происходит в две стадии. Первая – это холодное заполнение полостей в прототипе порошковым материалом или его смесью с водой. В качестве тестового материала был выбран порошок титана, хотя предлагаемая технология подразумевает возможность использования широкого спектра порошковых материалов – как металлических, так и керамических. Вторая стадия – последующий отжиг. При этом происходят удаление полимера и спекание металлического порошка с сохранением исходной формы и размеров прототипа. Термическая обработка полученных прототипов проводилась как в атмосфере аргона, так и при свободном доступе атмосферного воздуха. Использование различных газовых сред может приводить к протеканию химических преобразований в составе материала, заполняющего прототип. Проведенные эксперименты позволяют сделать вывод о перспективности дальнейшего технологического развития представленных подходов. Также не исключается возможность соединения двух рассмотренных способов в один для достижения оптимального конечного результата. Полученные данные могут способствовать расширению области использования стереолитографических установок – наиболее точных, распространенных и доступных машин на данный момент из широкого типа аддитивных аналогов.

Ключевые слова: аддитивные технологии, титановый порошок, 3D-модель, спекание

Благодарности: Работа проведена в рамках выполнения государственного задания НИЦ «Курчатовский институт».

Для цитирования: Марков М.А., Черобыло С.А., Ипполитов Е.В., Камаев С.В., Новиков М.М., Внук В.В. Преобразование стереолитографических прототипов в металлические или керамические модели замещением полимера порошковым титаном. *Известия вузов. Порошковая металлургия и функциональные покрытия*. 2024;18(2):61–70.
<https://doi.org/10.17073/1997-308X-2024-2-61-70>

Introduction

Additive manufacturing using various materials finds widespread application across diverse fields. The list of such technologies and materials continually expands with the addition of new items [1–8]. Laser stereolithography, employed in photocurable polymers, stands out as one of the most extensively used additive technologies due to its diverse material options and a wide price range for equipment, ranging from costly industrial machines to affordable household devices. This equipment demonstrates the capability to produce highly accurate objects.

Converting polymer prototypes into metal or ceramic components requires specific equipment and skilled personnel, such as through methods like molding or cavityless casting.

In the realm of additive manufacturing for ceramic models, several noteworthy technological implementations exist. These include layer-by-layer sintering of powder ceramics, curing of photopolymerizing compositions with ceramic fillers, and local extrusion of ceramic-filled material [2–6]. Notably, these technologies involve high-temperature processing stages to eliminate the polymer binder, achieve surface gloss, conduct additional pore-filling impregnation, among other steps. Regarding additive manufacturing of metal models, methods encompass layer-by-layer sintering of metal powders, layer-by-layer model formation via polymerization of filled compositions, and local extrusion of filled material (followed by sintering) [4–12].

This paper explores the potential expansion of the application scope for stereolithography equipment that work with photopolymers. It specifically examines new possibilities for converting prototypes into ceramic or metal parts.

Experimental part

In our view, one solution to broaden the applicability of stereolithography involves producing polymer stereolithographic parts with available free volume. Such models could undergo subsequent cold filling with ceramic or metal powder, followed by heat treatment to eliminate the polymer component of the model (referred to as annealing) and the sintering of metal or ceramics (henceforth referred to as “sintering” without separately delineating the polymer burnout process).

During sintering, there is potential to synthesize a ceramic compound from the substance used to fill the model body [13; 14]. The sintering stage in this technology shares similarities with the method utilizing filled resins.

We have explored two straightforward methods to create models suitable for subsequent filling with alternate materials. These methods involve producing a thin-walled inverse fillable model, essentially a matrix, and a contourless model exhibiting significant free volume uniformly distributed throughout its body.

The process of obtaining the inverse model, or matrix, is depicted in Fig. 1. In this developed model, a matrix is created by indenting the working surface of the model by a specified thickness. The design incorporates a port for powder filling and includes a covering lid as integral parts.

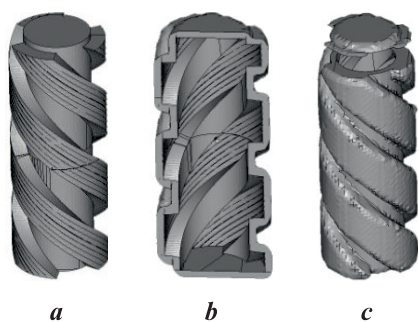


Fig. 1. Stages of part matrix construction for powder filling with sintered material

a – initial model, *b* – hollow matrix (sectional view), *c* – model displaying the matrix with a separated closing lid

Рис. 1. Построение матрицы модели для заполнения ее порошком спекаемого материала
a – исходная модель, *b* – пустотелая матрица (в разрезе),
c – модель матрицы с отделенной крышкой

This alternative approach shares some resemblance to sintering within a non-burnable mold [15]. However, in our scenario, the mold is combustible, and its intricacy is solely constrained by the designer’s capabilities. In place of matrix models, we suggest employing original contourless prototypes. When creating a typical stereolithographic part, the process involves outlining both external and internal contours while filling the space between them. Additionally, denser outer hatching is necessary for horizontal outer surfaces.

To implement the contourless technology in stereolithography, several modifications to the conventional process are required, such as:

- eliminating contours;
- removing denser outer hatching;
- using only one coordinate (either *X* or *Y*) on each layer; the direction of hatching alternates through the layer;
- increasing the hatching step.

The sparse hatching serves as an internal frame structure that gets filled with the initial liquid resin during manufacturing. By the end of the process, the liquid resin naturally flows out from the model or is expelled by compressed air.

Fig. 2 illustrates both the conventional method and the validated contourless methods for creating a stereolithographic part of a cylinder.

The model produced using this technology adopts a cellular polymer structure, openly accessible on all sides, containing a uniformly distributed free volume internally. Experimental findings indicate that manipulating technological parameters, such as layer thickness (*h*) and hatching step (*H_s*), within the ranges

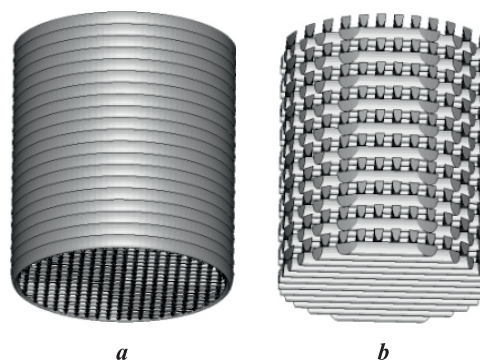


Fig. 2. The models fabricated via conventional (contour + *X*–*Y* hatching) (*a*) contourless (alternating *X* and *Y* hatching layer by layer) (*b*) stereolithography techniques

Рис. 2. Вид моделей, полученных по традиционной стереолитографической технологии (контуры + штриховка *X*–*Y*) (*a*) и бесконтурно, с чередующейся через слой штриховкой *X* и *Y* (*b*)

of $h = 100$ to $200 \mu\text{m}$ and $H_s = 0.5$ to 0.9 mm , results in varying proportions of free volume within the model, ranging from 30 to 80 %. A designer can replicate a similar internal hollow structure that fills the model. However, in such cases, the model's complexity significantly impacts the file size, potentially increasing it by several orders of magnitude. This could pose challenges for subsequent software processing to prepare the model for printing, potentially rendering it difficult or even impossible. In contrast, contourless models achieve the same effect by simply adjusting the model growing technology without burdening the file size with excessive complexity.

We opted for titanium powder with particle sizes ranging from 15 to $45 \mu\text{m}$ to explore the replacement of prototype material. Titanium is highly sought-after in engineering and medical applications. Additionally, both titanium and previously used silicon can serve as intermediate materials capable of forming ceramic compounds (such as nitride, oxide, and carbide) under suitable conditions, offering a wide array of structural properties [17–19].

The matrix models were dry-filled through the open facet, followed by sealing the closing lid with initial resin cured under a UV lamp.

For the filling of contourless models, a suspension of titanium powder and water was prepared. Filling the free volume in the models was conducted within an MK-mini vacuum chamber ("MK-Technology," Germany). Experimental findings revealed optimal results when the filler constituted approximately $50 \pm 5 \text{ vol. \%}$ of the suspension.

Subsequently, all samples underwent heat treatment. Both matrix and contourless models were sintered under similar conditions using an SUOL-0.25.1/12-I1 furnace (manufactured in Russia). Sintering temperatures ranged from 900 to $1200 \text{ }^\circ\text{C}$. The process was executed with gas purging (argon, nitrogen) and with

exposure to atmospheric air. Sintering durations did not exceed 10 min.

Experimental results

Fig. 3 displays photographs of the test contourless models captured at various stages of the technological process.

The model obtained after sintering remarkably retained its original shape and dimensions, showcasing the initial color of the titanium powder and exhibiting adequate mechanical strength and electrical conductivity. The furnace utilized in our experimentation is well-suited for gas purging (specifically, Ar and N_2 in our case) and effectively prevents the temperature from exceeding $1200 \text{ }^\circ\text{C}$. When using Ar purging, a minor quantity of weakly sintered metal powder (forming a loose layer up to 100 microns thick) was observed on the surface of the models. Sintering conducted at lower temperatures (1000 and $1100 \text{ }^\circ\text{C}$) also yielded integral samples, albeit with inferior surface quality. Considering that the melting temperature of titanium is $1670 \text{ }^\circ\text{C}$, it can be inferred that elevated temperatures might enhance the final model's quality.

As previously mentioned, the resulting samples exhibited the same colour as the original metal powder. Sintering the Ti-polymer model in an argon environment may instigate a reaction between titanium and the polymer of the initial prototype. Under such conditions, stoichiometric titanium carbide TiC , which conducts electrical current similar to Ti, can be formed, along with several non-stoichiometric carbides, such as Ti_xC_y [19; 20]. According to literature sources, titanium actively reacts with atmospheric gases like nitrogen and oxygen at high temperatures. This reaction results in the formation of titanium nitride and titanium oxide, respectively. It's essential to note that not only metallic titanium but also its compounds, such as carbides and nitrides, have the potential to interact with oxygen [18–22].



Fig. 3. Contourless samples

a – stereolithographic contourless model; *b* – the same model filled with titanium-water suspension;
c – the model after a 10 min sintering at $1200 \text{ }^\circ\text{C}$ under argon purging

Рис. 3. Тестовые бесконтурные образцы

a – стереолитографическая бесконтурная модель; *b* – та же модель, заполненная титановодяной суспензией;
c – модель после 10 мин спекания при $t = 1200 \text{ }^\circ\text{C}$ с продувкой аргоном

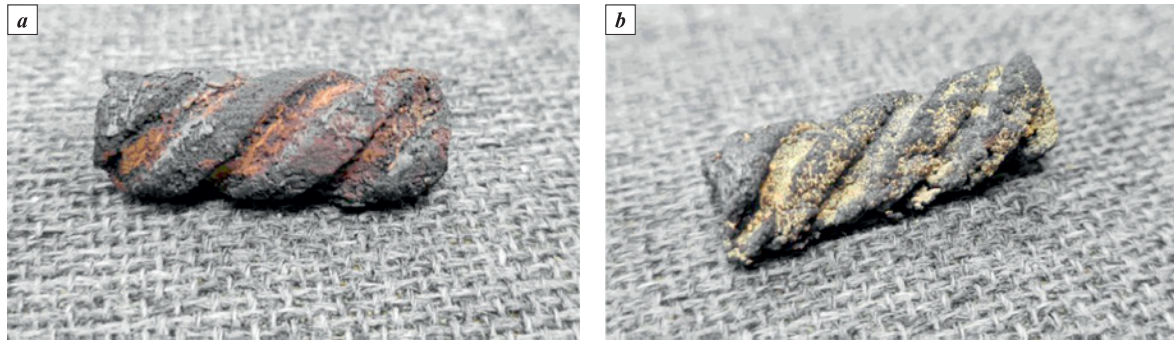


Fig. 4. Counterless samples following heat treatment at $t=1100\text{ }^{\circ}\text{C}$ under nitrogen purging (a) and in atmospheric air (b)

Рис. 4. Тестовые бесконтурные образцы после проведения спекания при $t = 1100\text{ }^{\circ}\text{C}$ с продувкой азотом (a) и в атмосферном воздухе (b)

Sintering the contourless models in a nitrogen environment resulted in samples that maintained the original shape and dimensions, akin to the experiments conducted in argon. These samples exhibited electrical conductivity, although at times, surface cleaning was necessary to verify this property. Both titanium nitride and titanium carbide act as metal-type conductors, particularly in the case of stoichiometric TiN or TiC compounds, while TiO_2 oxide functions as a dielectric material [23–25].

Sintering in a nitrogen environment imparted a reddish-brown color to the samples, characteristic of titanium nitride TiN (Fig. 4, a). However, upon discontinuing nitrogen purging and before the samples cooled completely, a layer of white or yellow color formed on their surfaces, typical of titanium oxide TiO_2 . Fig. 4, b illustrates a sample obtained through heat treatment in atmospheric air. Both samples (Fig. 4, a, b) displayed a slightly molten surface, which is noticeable when compared with the sample in Fig. 3, c. According to reference data [26], the enthalpies of titanium dioxide and nitride

formation are $\Delta H_f^{\circ} = -944 \div -938\text{ kJ/mol}$ (for different modifications) and $\Delta H_f^{\circ} = -323\text{ kJ/mol}$, respectively. During sintering, after the removal of the polymer, the structure of the samples was notably porous, displaying a branched surface. Due to chemical reactions, the temperature on their surface increased, resulting in localized areas of melted material.

The matrix models underwent a sintering process akin to the previously described sintering of contourless prototypes. Fig. 5 illustrates the stages of sample preparation and the outcome of sintering with argon purging.

A layer of orange-colored substance developed on the surface of the sintered model, particularly noticeable on the protruding sections. A similar occurrence was observed on the contourless models with nitrogen purging, albeit in the recessed areas. The models generated in this manner, depicted in Fig. 5, c, more faithfully replicate the shape of the original model. Structurally, they also exhibit strength, and the orange layer can be removed from the surface using abrasive

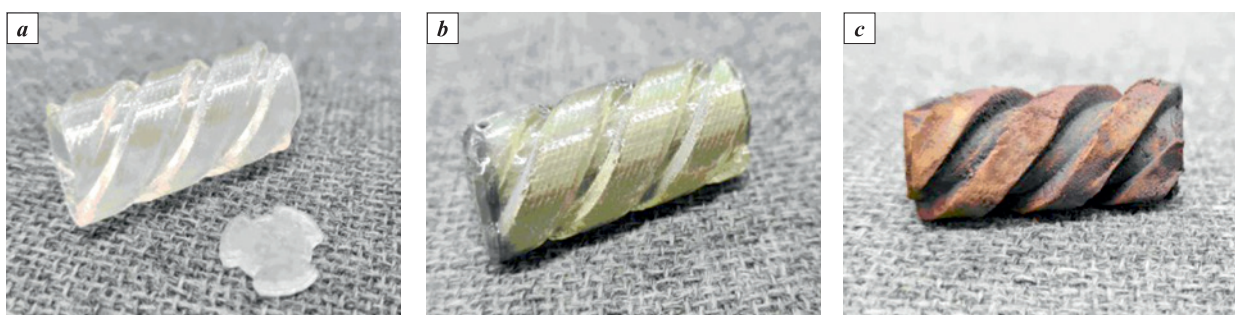


Fig. 5. Matrix samples

a – stereolithographic part depicting a component matrix with a lid; b – sealed matrix filled with titanium powder; c – the sample after a 10 min sintering at $1200\text{ }^{\circ}\text{C}$ under argon purging

Рис. 5. Тестовые матричные объекты

a – стереолитографическая модель матрицы объекта с крышкой; b – заклеенная матрица, заполненная титановым порошком; c – образец после 10 мин спекания при $t = 1200\text{ }^{\circ}\text{C}$ с продувкой аргоном

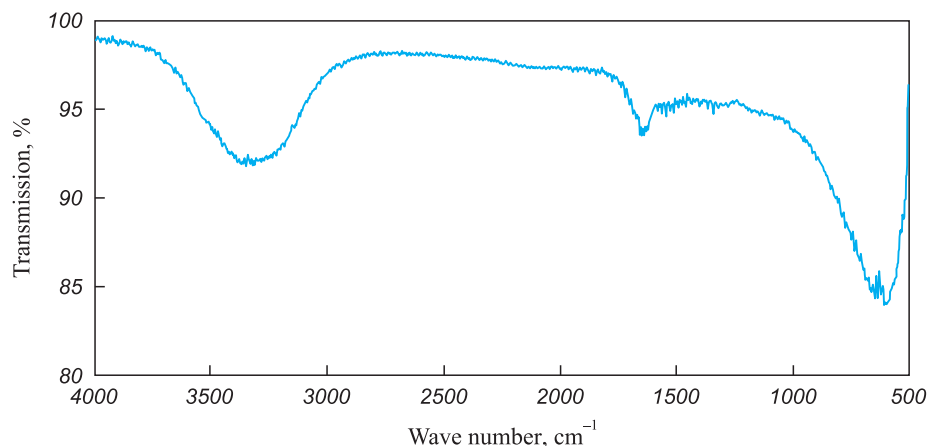


Fig. 6. FTIR spectrum analysis of substance from outer protruding parts of sintered matrix sample surface following 10 min sintering at 1200 °C under argon purging

Рис. 6. FTIR спектр вещества с внешних выступающих частей поверхности матричного образца после 10 мин спекания при $t = 1200$ °C с продувкой аргоном

materials or tools. Post-removal, the sample adopts a grey hue, akin to titanium powder.

Spectroscopy (FTIR) of the substance extracted from the surface of matrix models indicated (Fig. 6) the closest resemblance to the spectrum of non-stoichiometric Ti_3C_2 carbide. Notably, the spectrum obtained lacked characteristic lines indicative of Ti–N bonds [19; 27–34].

Figs. 7 and 8 depict matrix samples sintered under nitrogen purging and in an air environment, respectively. In the case of nitrogen purging, the samples sintered in this medium exhibited a more oxidized surface compared to those sintered in an air environment. The matrix samples prepared for sintering were densely packed with metal powder, as previously described. The metal was encapsulated from the surrounding medium by the matrix itself, formed by a layer of cured polymer. Heating initiated the thermal decomposition

or combustion of the polymer, prompting the metal to react with the resulting decomposition products. Previous findings indicated that in an inert argon environment, this led to the formation of a layer composed of titanium-carbon compounds on the surface. As the polymer layer burned out, it gradually thinned and became permeable to atmospheric air or other gases, initiating competing processes between the formation of titanium carbide and titanium nitride [35; 36]. Titanium nitride reacted with heavier products of polymer thermal decomposition, containing a significant oxygen content, and transformed into oxide. It's noteworthy that oxidation of titanium nitride commences at lower temperatures compared to titanium carbide. The simultaneous occurrence of these exothermic reactions on the sample surface induced additional heating and surface melting, irrespective of the temperature used for heat treatment (refer to Fig. 7).

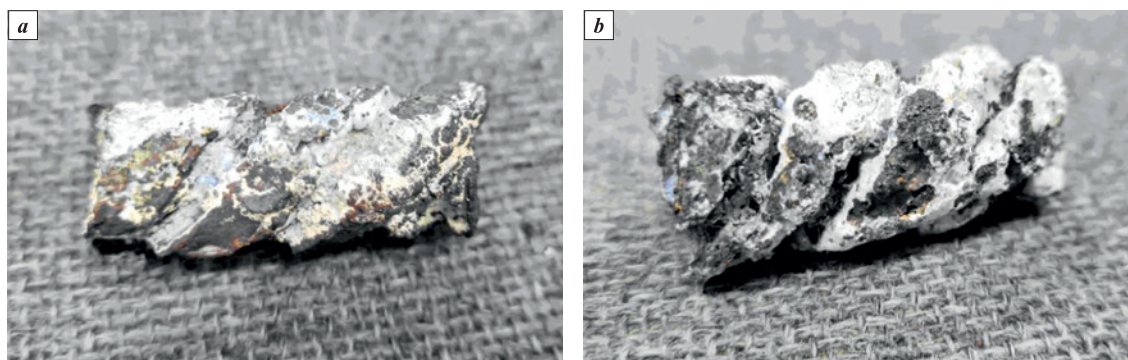


Fig. 7. Matrix samples following sintering under nitrogen purging at $t = 1000$ °C (a) and 1200 °C (b)

Рис. 7. Тестовые матричные образцы после спекания с продувкой азотом при $t = 1000$ °C (a) и 1200 °C (b)



Fig. 8. Matrix samples following sintering in air at $t = 900\text{ °C}$ (a), 1000 °C (b) and 1100 °C (c)

Рис. 8. Тестовые матричные образцы после спекания на воздухе при $t = 900\text{ °C}$ (a), 1000 °C (b) и 1100 °C (c)

Samples sintered in atmospheric air (Fig. 8) exhibited distinct differences from those treated with nitrogen purge. One notable characteristic was their sensitivity to the sintering temperature: lower temperatures (within specific limits) resulted in better retention of the sample's shape and a cleaner surface. Moreover, these samples, despite exposure to atmospheric oxygen, showed minimal amounts of generated titanium oxide, observed only at temperatures surpassing 1100 °C .

We hypothesize that such sintering behavior can be elucidated by the fact that in the presence of atmospheric oxygen, the polymer matrix underwent combustion rather than decomposition. The primary combustion products (H_2O and CO_2) were not retained on the surface of the sintered sample. Additionally, the outflow of hot gaseous combustion products from the reaction area hindered the entry of nitrogen and oxygen. Combustion of the polymer also resulted in a decreased presence of carbide on the titanium surface. Notably, at a sintering temperature of 900 °C , the samples with the cleanest surfaces, in comparison to others, were produced.

Results and discussion

Fig. 9 presents cross-sectional photos of the sintered samples purged with argon. The contourless sample retained a mesh structure at the edges, inverse to that of the original prototype. In the center, there's an area of sintered powder characterized by discontinuous pinpoint metallic luster. The matrix sample exhibited a darker outer layer, while the rest of the sample displayed a shiny metal appearance.

These investigations validate the feasibility of producing 3D metal models using a stereolithography apparatus, without necessitating foundry technologies. Each of the alternative technologies presented here holds distinct characteristics to be considered during the development of a final technological solution. Selecting a viable solution should follow a phase of experiments and tests evaluating the strength of the model.

All models created using the described methods required post-processing to eliminate the outer layer of the material. This post-processing step should be factored in during the computer modeling phase.

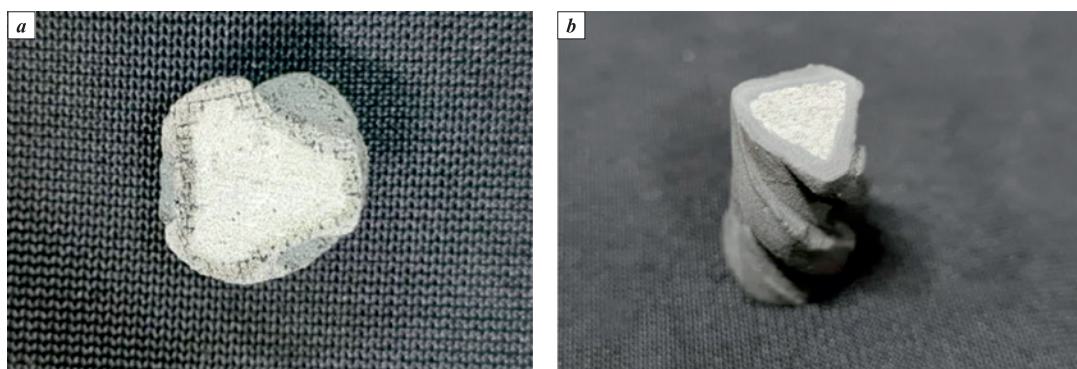


Fig. 9. Cross-sections of a sample sintered at $t = 1000\text{ °C}$
a – contourless sample; b – matrix sample

Рис. 9. Срезы образцов, спеканных при $t = 1000\text{ °C}$
a – бесконтурный образец; b – матричный образец

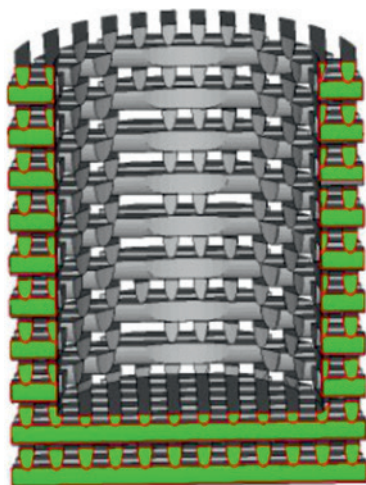


Fig. 10. Cross-section of a cylindrical sample model with contourless shell and internal cavity for metal powder or suspension filling

Рис. 10. Модель цилиндрической детали в разрезе, имеющая бесконтурную оболочку и внутреннюю полость для последующего заполнения металлическим порошком или суспензией

We are intrigued by the prospect of merging contourless and matrix technologies into one by creating a contourless matrix (as shown in Fig. 10). The wall of such a matrix is anticipated to be filled with a metal-water suspension, while the inner cavity may be filled either with dry powder or the same suspension. By selecting an appropriate sintering mode that facilitates easy removal of the weakly sintered outer porous part, the final model will resemble a sintered powder devoid of channels from polymer elements, minimizing its contact with external media during sintering.

Conclusions

Therefore, our experiments have validated the feasibility of transforming stereolithographic prototypes into metal or metal-ceramic forms. Through the use of titanium as an exemplary material, we have effectively showcased the genuine potential for such a transformation. By employing the described prototypes, we expand the utility of stereolithography, enhancing its versatility. Notably, the proposed solution does not necessitate any alterations to the photopolymer.

In contrast to additive technologies applied to metals or ceramics, which typically involve the use of significantly more expensive equipment, stereolithography equipment has consistently stood out as one of the most precise and user-friendly types of additive technology.

Additionally, it's noteworthy that the methods we propose facilitate the manufacturing of models with varying degrees of porosity. This aspect holds sig-

nificance in both technical and medical applications of such models.

References / Список литературы

- Jacobs P.F. Introduction to rapid prototyping and manufacturing. rapid prototyping and manufacturing: Fundamentals of stereolithography. 1st ed. Dearborn, MI, USA: Society of Manufacturing Engineers, 1992. 434 p
- Baumers M., Dickens P., Tuck C., Hague R. The cost of additive manufacturing: machine productivity, economies of scale and technology-push. *Technological Forecasting and Social Change*. 2016;102:193–201. <https://doi.org/10.1016/j.techfore.2015.02.015>
- Bartolo P.J., Gaspar J. Metal filled resin for stereolithography metal part. *CIRP Annals-Manufacturing Technology*. 2008;57(1):235–238. <https://doi.org/10.1016/j.cirp.2008.03.124>
- Colombo P., Mera G., Riedel R., Soraru G.D. Polymer-derived ceramics: 40 years of research and innovation in advanced ceramics. *Journal of the American Ceramic Society*. 2010;93(7):1805–1837. <https://doi.org/10.1002/9783527631940.ch57>
- Rice R.W. Ceramic fabrication technology. New York: CRC Press, 2003. 362 p.
- Gonzalez-Gutierrez J., Cano S., Schuschnigg S., Kukla C., Sapkota J., Holzer C. Additive manufacturing of metallic and ceramic components by the material extrusion of highly-filled polymers: A review and future perspectives. *Materials*. 2018;11(5):840. <https://doi.org/10.3390/ma11050840>
- Popovich A., Sufiarov V. Metal powder additive manufacturing. *New Trends in 3D Printing*. 2016;215–236. <https://doi.org/10.5772/63337>
- DebRoy T., Wei H.L., Zubuck J.S., Mukherjee T., Elmer J.W., Milewski J.O., Beese A.M., Wilson-Heid A., Zhang A.W. Additive manufacturing of metallic components – Process, structure and properties. *Progress in Material Science*. 2018;92:112–224. <https://doi.org/10.1016/j.pmatsci.2017.10.001>
- Halloran J. W., Griffith M., Chu T-M. Stereolithography resin for rapid prototyping of ceramics and metals: Patent 6117612A (USA).1997.
- Mireles J., Espalin D., Roberson D., Zinniel B., Medina F., Wicker Fused R. Fused deposition modeling of metals. In: *Proceedings of 23rd Annual International Solid Freeform Fabrication Symposium. An Additive Manufacturing Conference* (Austin Texas, 6–8 August 2012). 2012. P. 836–845.
- Liu B., Wang Y., Lin Z., Zhang T. Creating metal parts by fused deposition modeling and sintering. *Materials Letters*. 2020;263:127252. <https://doi.org/10.1016/j.matlet.2019.127252>
- Giberti H., Strano M., Annoni M. An innovative machine for fused deposition modeling of metals and advanced ceramics. In: *MATEC Web of Conferences (4th International Conference on Nano and Materials Science)*. 2016;43: 1–5. <https://doi.org/10.1051/mateconf/20164303003>
- Vnuk V.V., Ippolitov E.V., Kamaev S.V., Markov M.A., Novikov M.M., Cherebylo S.A. Investigation of the pro-

- cess of laser photopolymerization of composite materials based on methacrylic oligomers and silicon powder. *Khimicheskaya fizika*. 2020;39(9):88–93. (In Russ.). <https://doi.org/10.31857/s0207401x20090137>
- Внук В.В., Ипполитов Е.В., Камаев С.В., Марков М.А., Новиков М. М., Черобыло С. А. Исследование процесса лазерной фотополимеризации композитных материалов на основе метакриловых олигомеров и порошка кремния. *Химическая физика*. 2020;39(9):88–93. <https://doi.org/10.31857/s0207401x20090137>
14. Markov M., Vnuk V., Ippolitov E., Kamayev S., Cherebylo S. The prospects for transforming stereolithographic parts from polymer to ceramic by using powder silicon as photocurable resin filler. *The International Journal of Advanced Manufacturing Technology*. 2020;111:1863–1871. <https://doi.org/10.1007/s00170-020-06239-0>
 15. Kiseev V.M. Napominayushchij A.S. Method of obtaining porous titanium: Patent RU2407817 (RF). 2010. (In Russ.). Кисеев В.М., Напоминающий А.С. Способ получения пористого титана: Патент RU2407817 (РФ). 2010.
 16. Evseev A.V., Lazaryanc V.E., Markov M.A., Mikhlin V.S., Surovtsev M.A., Fershtut E.V. Liquid photopolymerizing composition for laser stereolithography: Patent 2395827 (RF). 2008. (In Russ.). Евсеев А.В., Лазарянец В.Э., Марков М.А., Михлин В.С., Суворцев М.А., Ферштут Е.В. Жидкая фотополимеризующаяся композиция для лазерной стереолитографии: Патент 2395827 (РФ). 2008.
 17. Gotman I., Gutmans E.Y. Titanium nitride-based coatings on implantable medical devices. *Advanced Biomaterials and Devices in Medicine*. 2014;1:53–73.
 18. Shabalin I.L., Roach D.L. Oxidation of titanium carbide-graphite hetero-modulus ceramics with low carbon content: I. Phenomenological modeling of the ridge effect. *Journal of the European Ceramic Society*. 2008;28(16):3165–3176. <https://doi.org/10.1016/j.jeurceramsoc.2008.04.035>
 19. Li Y., Zhou X., Wang J., Deng Q., Li M., Du S., Han Y-H., Lee J., Huang Q. Facile preparation of *in situ* coated $Ti_3C_2T_x/Ni_{0.5}Zn_{0.5}Fe_2O_4$ composites and their electromagnetic performance. *RSC Advances*. 2017;7(40):24698–24708. <https://doi.org/10.1039/C7RA03402D>
 20. Lee J.-Y., Jo W.-K. Control of methyl tertiary-butyl ether via carbon-doped photocatalysis under visible-light irradiation. *Environmental Engineering Research*. 2012;12(4):179–184. <https://doi.org/10.4491/eer.2012.17.4.179>
 21. Gray B.M., Hector A.L., Jura M., Owen J.R., Whittam J. Effect of oxidative surface treatments on charge storage at titanium nitride surface for super capacitor applications. *Journal of Materials Chemistry: A*. 2017;5(9):4550–4559. <https://doi.org/10.1039/C6TA08308K>
 22. Pambudi A.B., Kurniawati R., Iryani A., Hartanto D. Effect of calcination temperature in the synthesis of carbon doped TiO_2 without external carbon source. In: *The 3rd International Seminar on Chemistry: AIP Conference Proceedings, 2018* (Surabaya, Indonesia, 18–19 July 2018). P. 020074. <https://doi.org/10.1063/1.5082479>
 23. Ishkov A.V., Sagalakov A.M. Electric conductivity of composites containing nonstoichiometric titanium compounds. *Technical Physics Letters*. 2006;32(5):377–378. <https://doi.org/10.1134/S1063785006050038>
 24. Ghidui M., Lukatskaya M.R., Zhao M.-Q., Gogots Y.i, Barsoum M. Conductive two-dimensional titanium carbide “clay” with high volumetric capacitance. *Nature*. 2014;516(7529):78–81. <https://doi.org/10.1038/nature13970>
 25. Andrievskii R.A., Alekseev S.A., Dzodziev G.T., Dzenladze A.Z., Travushkin G.G., Turchin V.N., Chertovich A.F. Physicomechanical properties of titanium carbide with titanium nitride additions. *Soviet Powder Metallurgy and Metal Ceramics*. 1980;19:612–615.
 26. Chemical encyclopedia. Vol. 4. Moscow: Bolshaya rossiyskaya encyclopedia, 1995. P. 1176–1178. (In Russ.). Химическая энциклопедия. Т. 4. Москва: Большая российская энциклопедия, 1995. С. 1176–1178.
 27. Chen C., Liu F., Li S., Wang N., Popov A., Jiao M., Wei T., Li Q., Dunsch L., Yang S. Titanium/yttrium mixed metal nitride clusterfullerene $TiY_2N@C80$: synthesis, isolation, and effect of the group-III metal. *Inorganic Chemistry*. 2012;51:3039–3045. <https://doi.org/10.1021/ic202354u>
 28. Wang X.B., Ding C.F., Wang L.S. Vibrational resolved photoelectron spectra of TiC_x^- ($x = 2-5$) clusters. *The Journal of Physical Chemistry: A*. 1997;101(42):7699–7701. <https://doi.org/10.1021/jp971838k>
 29. Snyder M.Q., McCool B.A., DiCarlo J., Tripp C.P., Desisto W. An infrared study of the surface chemistry of titanium nitride atomic layer deposition on silica from $TiCl_4$ and NH_3 . *Thin Solid Films*. 2006;514(1-2):97–102. <https://doi.org/10.1016/j.tsf.2006.03.013>
 30. Leon A., Reuquen P., Garin C., Segura R., Vargas P., Zapata P., Orihuela P. FTIR and Raman characterization of TiO_2 nanoparticles coated with polyethylene glycol as carrier for 2-methoxyestradiol. *Applied Sciences*. 2017;7(49):1–9. <https://doi.org/10.3390/app7010049>
 31. Foratirad H., Baharvandi H.R., Maragheh M.G. Rheological behavior of aqueous titanium carbide suspension and evaluation of the gelcasted green body properties. *Material Research*. 2017;20(1):175–182. <https://doi.org/10.1590/1980-5373-MR-2016-0410>
 32. Schramke K., Qin Y., Held J.T., Mkhoyan K.A., Kortshagen U. Nonthermal plasma synthesis of titanium nitride nanocrystals with plasmon resonances at near-infrared wavelength relevant to photothermal therapy. *ACS Applied Nano Materials*. 2018;1:2869–2876. <https://doi.org/10.1021/acsnanm.8b00505>
 33. Spectra base. URL: <https://spectrabase.com/spectrum/IKP1d7RLMfa> (accessed: 18.05.2023).
 34. Kaviyarasu K., Thema F.T., Manikandan E., Maaza M. TiO_2 doped graphene oxide (GO) wrinkle nanosheets by wet-chemical method. *Synthesis and Reactivity in Inorganic, Metal-Organic, and Nano-Metal Chemistry*. 2016;7129:722.
 35. Jiao K., Zhang J., Liu Z., Kuang S., Liu Y., Liu F. Dissection investigation of $Ti(C,N)$ behavior in blast furnace hearth during vanadium titanomagnetite smelting. *ISIJ International*. 2017;57(1):48–54. <https://doi.org/10.2355/isijinternational.ISIJINT-2016-419>
 36. Wang B., Matsumaru K., Ishiyama H., Yang J., Ishizaki K., Matsushita J. Low temperature oxidation of titanium nitride under high oxygen pressure by O_2 -HIP. In: *Proc. International Conference on Hot Isostatic Pressing Kobe* (Japan, 12–14 April 2011). *Journal of Materials online*. <https://doi.org/10.2240/azojomo0308>

Information about the Authors




Mikhail A. Markov – Researcher, National Research Centre “Kurchatov Institute”

 **ORCID:** 0000-0003-1054-2615


 **E-mail:** Lc250@mail.ru

Svetlana A. Cherebylo – Researcher, National Research Centre “Kurchatov Institute”

 **ORCID:** 0000-0003-0502-9681

 **E-mail:** Svetlana.cherebylo@rambler.ru

Evgeniy V. Ippolitov – Researcher, National Research Centre “Kurchatov Institute”

 **ORCID:** 0000-0002-0622-6727


 **E-mail:** ippevg@yandex.ru

Sergey V. Kamaev – Researcher, National Research Centre “Kurchatov Institute”

 **ORCID:** 0000-0001-7423-1264

 **E-mail:** ksv6@rambler.ru

Mikhail M. Novikov – Senior Researcher, National Research Centre “Kurchatov Institute”

 **ORCID:** 0000-0003-0626-793X

 **E-mail:** novikov@rambler.ru

Vyacheslav V. Vnuk – Junior Researcher, National Research Centre “Kurchatov Institute”

 **ORCID:** 0000-0003-2536-6626

 **E-mail:** ren651@mail.ru

Сведения об авторах

Михаил Александрович Марков – науч. сотрудник, Федеральное государственное бюджетное учреждение «Национальный исследовательский центр «Курчатовский институт»

 **ORCID:** 0000-0003-1054-2615

 **E-mail:** Lc250@mail.ru

Светлана Александровна Чербыло – науч. сотрудник, Федеральное государственное бюджетное учреждение «Национальный исследовательский центр «Курчатовский институт»

 **ORCID:** 0000-0003-0502-9681


 **E-mail:** Svetlana.cherebylo@rambler.ru

Евгений Викторович Ипполитов – науч. сотрудник, Федеральное государственное бюджетное учреждение «Национальный исследовательский центр «Курчатовский институт»

 **ORCID:** 0000-0002-0622-6727

 **E-mail:** ippevg@yandex.ru

Сергей Валентинович Камаев – науч. сотрудник, Федеральное государственное бюджетное учреждение «Национальный исследовательский центр «Курчатовский институт»

 **ORCID:** 0000-0001-7423-1264

 **E-mail:** ksv6@rambler.ru

Михаил Михайлович Новиков – ст. науч. сотрудник, Федеральное государственное бюджетное учреждение «Национальный исследовательский центр «Курчатовский институт»

 **ORCID:** 0000-0003-0626-793X

 **E-mail:** novikov@rambler.ru

Вячеслав Владимирович Внук – мл. науч. сотрудник, Федеральное государственное бюджетное учреждение «Национальный исследовательский центр «Курчатовский институт»

 **ORCID:** 0000-0003-2536-6626

 **E-mail:** ren651@mail.ru

Contribution of the Authors



M. A. Markov – contributed to computer model development, participated in conducting experiments, discussions of results, and paper writing.

S. A. Cherebylo – conducted experiments related to the stereolithographic component, contributed to paper writing.

E. V. Ippolitov – conducted experiments involving model preparation and the heat treatment stage, participated in result discussions.

S. V. Kamaev – contributed to result discussions and paper writing.

M. M. Novikov – conducted experiments related to filling models with powder filler, participated in result discussions.

V. V. Vnuk – conducted experiments related to the heat treatment stage and spectroscopy.

Вклад авторов

М. А. Марков – разработка компьютерных моделей, участие в проведении экспериментов, обсуждении результатов и написании статьи.

С. А. Чербыло – проведение экспериментов (стереолитографическая часть), участие в написании статьи.

Е. В. Ипполитов – проведение экспериментов (подготовка моделей и термическая стадия), участие в обсуждении результатов.

С. В. Камаев – участие в обсуждении результатов, написании статьи.

М. М. Новиков – проведение экспериментов (заполнение моделей порошковым наполнителем), участие в обсуждении результатов.

В. В. Внук – проведение экспериментов (термическая стадия, спектроскопия).

Received 06.12.2022

Revised 19.07.2023

Accepted 21.07.2023

Статья поступила 06.12.2022 г.

Доработана 19.07.2023 г.

Принята к публикации 21.07.2023 г.